JACS
JOURNAL OF THE AMERICAN CHEMICAL SOCIETY
Communication
pubs.acs.org/JACS

Small Circular DNA Molecules Act as Rigid Motifs To Build DNA Nanotubes

Hongning Zheng, Minyu Xiao, Qin Yan, Yinzhou Ma, and Shou-Jun Xiao*

Nanjing National Laboratory of Microstructures, State Key Laboratory of Coordination Chemistry, School of Chemistry and Chemical Engineering, Nanjing University, Nanjing 210093, Jiangsu, China

Supporting Information

ABSTRACT: Small circular DNA molecules with designed lengths, for example 64 and 96 nucleotides (nt), after hybridization with a few 32-nt staple strands respectively, can act as rigid motifs for the construction of DNA nanotubes with excellent uniformity in ring diameter. Unlike most native DNA nanotubes, which consist of longitudinal double helices, nanotubes assembled from circular DNAs are constructed from lateral double helices. Of the five types of DNA nanotubes designed here, four are built by alternating two different rings of the same ring size, while one is composed of all the same 96-nt rings. Nanotubes constructed from the same 96-nt rings are 10−100 times shorter than those constructed from two different 96-nt rings, because there are fewer hinge joints on the rings.

The mechanical properties of small circular DNAs (tens to a hundred or more base pairs), such as bending, twisting, curving, kinking, stressing, rigidity, and disruption, have attracted scientists' great interest because they relate closely to the secret of our life—molecular mechanisms and functions of all kinds of DNA topological structures.[1] In addition, their molecular scale and geometry are well suited to mathematical topology model systems for quantitative analysis. From studies of the well-known wormlike model, such circular double-helix DNAs have been generally accepted to behave as rigid rings with smooth bending, i.e., small angular changes between the planes of adjacent base pairs, in solution over decades.[2] From another side, DNA nanotechnology pioneered by N. D. Seeman is based on rigid DNA motifs as building blocks to construct zero-, one-, two-, and three-dimensional (abbreviated as 0D, 1D, 2D, and 3D) nanostructures.[3] Here we address how small circular DNAs can act as rigid motifs to construct nanotubes, which are not yet as well-recognized in DNA nanotechnology as those made from linear strands. Such DNA minicircle-based nano-architecture might provide a new perspective for understanding the mechanical properties of circular DNAs.

In the early development stages, Seeman's group adopted a post-ligation strategy to close the nicking sites of polyhedral objects including cubes,[4] truncated octahedra,[5] and Borromean rings,[6] assembled from linear strands, which stabilized the flexible nanostructures when the DNAs were in their linear and end-open states. Similarly, Turberfield et al. constructed shape-persistent objects from DNA tetrahedra with high diastereoselectivity by post-ligation.[7] Another strategy employing small circular DNAs as rigid building blocks for DNA nano-architectures uses pre-circularized and purified DNAs directly in the assembly. Mao and co-workers used either circular or linear DNAs possessing the same sequence, for structural symmetry, to construct three- and four-arm building blocks and then hundreds of nanometer or micrometer 2D DNA network arrays.[8] Recently they also reported the use of circularized DNA as a "lid" to construct nanotubes with defined diameters and lengths.[9] In their designs, either circular or linear strands with the same sequence can replace each other without causing significant differences in the assembled nanostructural morphology. The explanation for this is that the core motifs in those designs are rigid tiles of double crossovers, and pairs of neighboring rigid tiles were connected with 4−9 thymines serving as hinges between them. Famulok et al. used DNA minicircles with gaps to construct rotaxane-like nano-robots and other nano-devices.[10] Sleiman et al. developed artificial DNA circles as motifs by inserting three or four rigid organic species to modify a small circular DNA into a triangle or a square, which then formed so-called lateral "rungs" that were linked longitudinally by double or single strands to construct DNA nanotubes.[11] The design benefits from the rigid lateral rungs consisting of rigid organic vertices and double-helix segments. Such chemically modified DNA strands could have potential applications in DNA self-assembly; however, they require laborious synthesis and purification, and again the artificial DNAs possess very different structures, making their assembly strategy somewhat different from that of native strands: e.g., the neighboring hinge joints "up" and "down" on lateral rungs were separated by a distance of two turns (21 base pairs (bp)), while the distance between two neighboring crossovers for origami built from native strands is 1.5 or 2.5 turns.

Herein, we report a new type of nanotubes assembled from native small circular DNAs, taking the advantage of the predicted rigidity of double-helix rings in solution. Two kinds of DNA single-stranded minicircles, with lengths of 96 and 64 nucleotides (nt), were used to demonstrate the feasibility of constructing geometrically well-defined DNA nanotubes of excellent uniformity from a few 32-nt staple strands without leaving a single base unpaired. Different from most previously reported native DNA nanotubes composed of longitudinal double helices, our nanotubes, assembled from circular DNAs,

Received: April 23, 2014
Published: July 7, 2014

dx.doi.org/10.1021/ja504050r | J. Am. Chem. Soc. 2014, 136, 10194−10197

are composed of lateral double helices. In all five of our designs (NT1−NT5), the circular single strands have bending, twisting, and kinking flexibility for hybridization with staple strands, and once these rings become completely double-helixed, they become rigid and can act as building blocks in DNA nanotechnology. The 32-nt complementary staple strands spanning two or three neighboring rings serve partly as building blocks when hybridized and partly as hinge joints when crossed over two or three neighboring rings to connect all the rings together. A vivid analogy for this kind of nanotubes is a tower constructed of kiss-stacked storeys.

The general approach to prepare small circular DNAs is enzymatic ligation. We applied T4 DNA ligase to close the nicking site with the help of a splint oligonucleotide (Supporting Information, Figure S1) and then purified the circularized DNAs by PAGE (Figures S2−S4).

Our first and second nanotube designs, NT1 and NT2, are depicted in Figure 1. The complete folding process for NT1

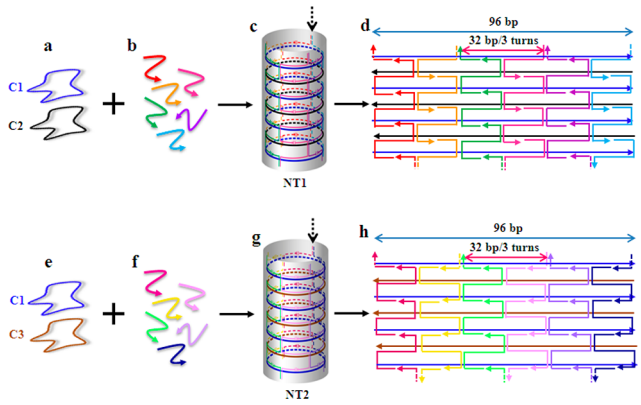

Figure 1. Folding strategies for the formation of nanotubes NT1 and NT2 from two 96-nt rings and six 32-nt complementary staple strands. (a) Cartoons of two 96-nt rings, with C1 in blue and C2 in black. (b) Six 32-nt staple strands shown in different colors. (c) Vivid 3D illustration of NT1. (d) Longitudinal section of NT1 with a breakline along the direction of the arrow in (c). (e) Cartoons of two 96-nt rings, C1 in blue and C3 in brown. (f) Six 32-nt staple strands shown in different colors. (g) Vivid 3D illustration of NT2. (h) Longitudinal section of NT2 with a breakline along the direction of the arrow in (g).

(Figure 1c) is illustrated in Figure 1a−d: two different 96-nt rings (C1 and C2, Figure 1a) are kiss-stacked anti-parallel to each other along the central axis, alternating six 32-nt staple strands (Figure 1b) to build NT1 (a vivid 3D illustration is shown in Figure 1c), a longitudinal section of which, with a breakline along the direction of the arrow shown in Figure 1c, is demonstrated in Figure 1d. Each 32-nt staple is divided into three concatenated parts—8 nt +16 nt + 8 nt—spanning three neighboring rings, and the long 16-nt sections from six staples are placed alternately on C1 and C2. According to the crossover rule in origami, the distance between two neighboring crossovers with opposite directions is 1.5 turns (or 16 bp); therefore, each ring bears six crossovers (96/16 = 6), which are designed to alternate in up and down directions.

For NT2, the long 16-nt sections from six staples are placed on the same ring (C3, Figure 1e). The complete folding process for NT2 (Figure 1g) is illustrated in Figure 1e−h. The folding strategy adopted here is similar to our previous reports[12] on folding rolling circle amplified DNAs or rolling circle transcripted RNAs with a few staple strands, except that in this case small circular DNA molecules replace the long single scaffolding DNA or RNA strands, and the resulting assembled nanostructures are nanotubes instead of nanoribbons.

Analyses of nanotubes NT1 and NT2 using atomic force microscopy (AFM) are demonstrated in Figure 2. Figure 2a−c

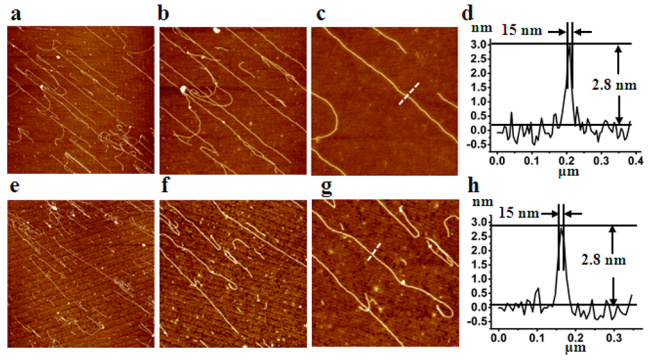

Figure 2. AFM characterization of nanotubes NT1 and NT2. (a−c) AFM images of NT1 from lower to higher magnification with image sizes at 12 × 12, 6 × 6, and 3 × 3 μm^2, where (b) is a zoom-in view of (a) and (c) is a zoom-in view of (b). (d) Cross-section profile of the dashed line in (c). (e−g) AFM images of NT2 from lower to higher magnification with image sizes at 14 × 14, 6 × 6, and 3 × 3 μm^2, where (f) is a zoom-in view of (e) and (g) is a zoom-in view of (f). (h) Cross-section profile of the dashed line in (g). Both (d) and (g) show the same height of 2.8 nm and the same width of 15 nm for NT1 and NT2.

reveals the well-defined DNA nanotubes NT1 from lower to higher magnification, with image sizes at 12 × 12, 6 × 6, and 3 × 3 μm^2, respectively, while Figure 2e−g presents NT2 at 14 × 14, 6 × 6, and 3 × 3 μm^2, respectively. Although the molecular structures of NT1 and NT2 are designed somewhat differently, their nanoscale morphologies in AFM look the same. The typical lengths of NT1 and NT2 are 3−15 μm. The cross-section analyses (Figure 2d,h) show a height of 2.8 nm and a width of 15 nm. Theoretically, the diameter of the tube can be easily calculated from the formula $d = C/\pi = (96 \times 0.34\ \text{nm})/\pi \approx 10$ nm for the nanotubes in the B-form duplex, where C represents the perimeter of the double-helix ring (96 × 0.34 nm ≈ 32 nm), 96 being the number of base pairs of the ring and 0.34 nm the length per base pair. Obviously, the measured height and width are not the parameters to describe such a nanotube. We executed AFM measurements in air within 8 h after DNA's adsorption on mica, during which time the nanotube lost water molecules and was squashed to a double layer. This squashed double layer has a width of around $C/2$ = 16 nm and a height of 2.8 nm (twice that of a double-helix DNA, 1.4 nm), corresponding very well to the measured dimensions.

Can we use only a single type of DNA ring molecules to cost-efficiently construct nanotubes? Figure 3 presents this as our third design: the same 96-nt rings (C1 in Figure 3a) are kiss-stacked anti-parallel to each other along the central axis by three 32-nt staple strands (Figure 3b) to build NT3 (Figure 3c). This kind of nanotubes could be constructed following the crossover rule of origami, with alternating crossovers at a distance of 1.5 turns (see Figure S7). However, according to the DNA strand displacement rule,[13] we suggest the folding structure of NT3 shown in Figure 3c as a vivid 3D view and in Figure 3d with a longitudinal section. Obviously only the

dx.doi.org/10.1021/ja504050r | J. Am. Chem. Soc. 2014, 136, 10194−10197

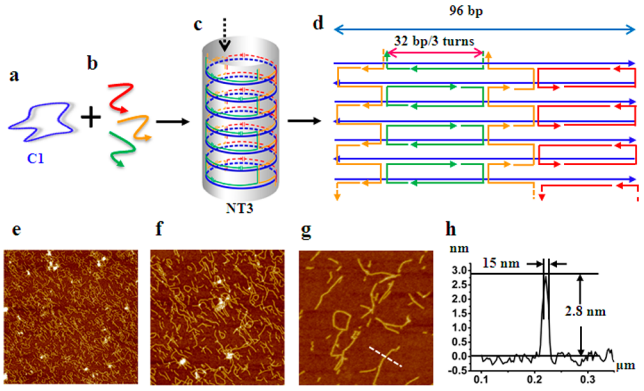

Figure 3. Construction of nanotube NT3 from C1 and 3 × 32 staple strands. (a) Cartoon of a single 96-nt ring of C1 in blue. (b) Three 32-nt staple strands shown in different colors. (c) Vivid 3D illustration of NT3. (d) Longitudinal section of NT3 with a breakline along the direction of the arrow in (c). (e–g) AFM images of NT3 from lower to higher magnification with image sizes at 6 × 6, 3 × 3, and 1 × 1 μm^2, respectively. (h) Cross-section profile of the dashed line in (g).

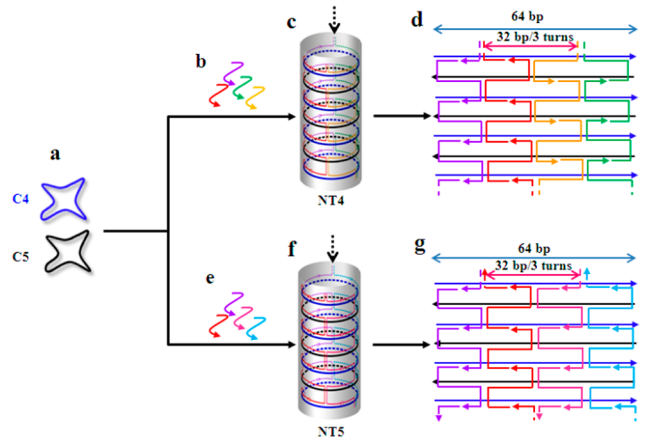

Figure 4. Folding strategies for the formation of nanotubes NT4 and NT5 from two 64-nt rings and four 32-nt complementary staple strands. (a) Cartoons of two 64-nt rings, with C4 in blue and C5 in black. (b) Four 32-nt staple strands shown in different colors. (c) Vivid 3D illustration of NT4. (d) Longitudinal section of NT4 with a breakline along the direction of the arrow in (c). (e) Four 32-nt staple strands shown in different colors. (f) Vivid 3D illustration of NT5. (h) Longitudinal section of NT5 with a breakline along the direction of the arrow in (g).

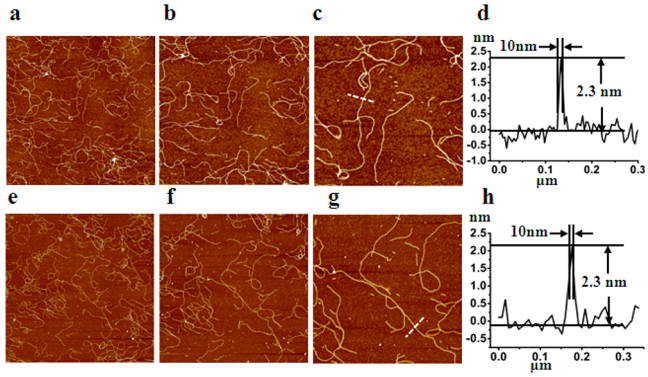

Figure 5. AFM characterization of nanotubes NT4 and NT5. (a–c) AFM images of NT4 from lower to higher magnification with image size at 9 × 9, 6 × 6, and 3 × 3 μm^2, respectively, where (b) is a zoom-in view of (a) and (c) is a zoom-in view of (b). (d) Cross-section profile of the dashed line in (c). (e–g) AFM images of NT5 from lower to higher magnification with image size at 9 × 9, 6 × 6, and 3 × 3 μm^2, respectively, where (f) is a zoom-in view of (e) and (g) is a zoom-in view of (f). (h) Cross-section profile of the dashed line in (g). Both cross-section profiles show the same height of 2.3 nm and the same width of 10 nm for NT4 and NT5.

orange 32-nt staple strand spans three neighboring rings, while the other two 32-nt staple strands (green and red) span two neighboring rings and form two 32-nt rectangles. In this case, each ring holds only four crossovers, which can be classified into two groups. Each group contains one up crossover and one down crossover at both hinge joints of the orange staples, and the two groups are separated by a green rectangle at one side and a red one at the other side.

AFM analyses in Figure 3e–g illustrate the typical length of nanotubes NT3 to be 100–500 nm, 10–100 times shorter than NT1 and NT2. A lot of nanotube fragments with length less than 100 nm are also observed. The cross-section profile in Figure 3h presents a height of 2.8 nm, i.e., a squashed bilayer of NT3, and a width of 15 nm, i.e., half the perimeter of NT3, which are the same as those of NT1 and NT2. The much shorter length of nanotubes NT3 proves the correct folding structure in Figure 3c,d because they have two fewer hinge joints on each ring than NT1 and NT2 and thus weaker binding to connect the rings together. To elaborate on the correct folding structure, we can look at it from the reverse side: according to the symmetry rule suggested by Mao,[9] if the nanotubes are folded as in Figure S7, they will be much longer than NT1 and NT2.

Next, we changed the ring size from 96 to 64 nt. Figure 4 illustrates the strategies for assembly of two 64-nt rings into nanotubes. Since the 64-nt ring can hold only four crossovers (64/16 = 4), two up and two down, only four 32-nt staple strands are needed for the assembly. Similar to NT1 and NT2, two different 64-nt rings (C4 and C5 in Figure 4a) are kiss-stacked anti-parallel to each other along the central axis, alternating four 32-nt staple strands (Figure 4b,e) to form NT4 (Figure 4c) and NT5 (Figure 4f). Figure 4d,g shows the corresponding longitudinal sections with a breakline along the arrow direction in NT4 or NT5, respectively. The only difference between NT4 and NT5 is that in NT5 all four long sections (16 nt) from the four 32-nt staples are placed on C5, while in NT4 the four long 16-nt sections from four 32-nt staples are allotted equally to C4 and C5.

AFM analyses in Figure 5 illustrate that the typical length of nanotubes NT4 and NT5 to be 0.5–3 μm. Cross-section analyses in Figure 5d,h show a height of 2.3 nm, i.e., a squashed bilayer of NT4 or NT5, and a width at 10 nm, i.e., half the perimeter of NT4 or NT5 [(64 × 0.34 nm)/2 = 11 nm], regardless of the type of folding. The diameters of NT4 and NT5 can be easily calculated as (64 × 0.34 nm)/$\pi \approx 7$ nm.

Can only a single type of 64-nt rings with two 32-nt staples be used to construct nanotubes, similar to NT3? According to the strand displacement rule, a single type of 64-nt rings more easily forms dimers with two anti-parallel rings instead of nanotubes with many interconnected rings.

As we expected, the nanotubes built from DNA minicircles are unique because they are constructed completely from lateral double helices only. The production yield is very high. Some unique characteristics of these nanotubes are emphasized: their diameter is geometrically well-defined with excellent uniformity; there are no open nanotubes with saw-tooth edges

dx.doi.org/10.1021/ja504050r | J. Am. Chem. Soc. 2014, 136, 10194–10197

as are often observed in nanotubes built from longitudinal double helices;[3h] circular DNAs are less degradable than linear DNAs in a physiological environment;[11] and they are well mono-dispersed but seldom aggregated together in solution. These unique properties might be preferable in biological technologies such as drug/gene delivery, gene up- and down-regulation, gene expression, and disease diagnosis and therapeutics.[14]

The successful assembly of nanotubes from small circular DNAs illustrates that the double-helix minicircles possess excellent rigidity for DNA nano-architectures. Meanwhile, the crossovers as hinge joints presents some bending flexibility and restricted torsional freedom in linking these small rings together. Both rigidity and bending flexibility need to be united to assemble the DNA minicircles into nanotubes. This work partly proves the power of predictions based on quantitative calculation of the topology from the experimental side. With further investigations, DNA minicircle-based nanotechnology will present a prosperous future.

■ ASSOCIATED CONTENT

Supporting Information

Experimental procedures, PAGE bands, sequence codes, design details, and more AFM images. This material is available free of charge via the Internet at http://pubs.acs.org.

■ AUTHOR INFORMATION

Corresponding Author

sjxiao@nju.edu.cn

Notes

The authors declare no competing financial interest.

■ ACKNOWLEDGMENTS

We are thankful for the financial support of NSFC, No. 91027019, the National Basic Research Program of China, No. 2013CB922101, and funding from the State Key Laboratory of Bioelectronics of Southeast University. Ziqi Lin is appreciated for providing the vivid 3D drawings.

■ REFERENCES

(1) For example, see: (a) Lederberg, J. *Physiol. Rev.* **1952**, *32*, 403. (b) *Mathematics of DNA Structure, Function and Interactions*; Benham, C. J., Harvey, S., Olson, W. K., Sumners, D. W., Swigon, D., Eds.; IMA Volumes in Mathematics and Its Applications *150*; Springer: Twin Cities, 2009. (c) Vologodskii, A. V. Circular DNA. Education Portal of the Biophysical Society, 1999; http://www.biophysics.org/portals/1/pdfs/education/vologodskii.pdf. (d) *Minicircle and Miniplasmid DNA Vectors*; Schleef, M., Ed.; Wiley-VCH: Weinheim, 2013. (e) Shore, D.; Langowski, J.; Baldwin, R. L. *Proc. Natl. Acad. Sci. U.S.A.* **1981**, *78*, 4833. (f) Shore, D.; Baldwin, R. L. *J. Mol. Biol.* **1983**, *170*, 957. (g) Crick, F. H.; Klug, A. *Nature* **1975**, *255*, 530. (h) Vologodskii, A.; Du, Q.; Frank-Kamenetskii, M. D. *Artif. DNA: PNA XNA* **2013**, *4*, 1. (i) Vafabakhsh, R.; Ha, T. *Science* **2012**, *337*, 1097. (j) Vologodskii, A.; Frank-Kamenetskii, M. D. *J. Am. Chem. Soc.* **2013**, *41*, 6785. (k) Zheng, X.; Vologodskii, A. *Biophys. J.* **2009**, *96*, 1341. (l) Du, Q.; Kotlyar, A.; Vologodskii, A. *Nucleic Acids Res.* **2008**, *36*, 1120. (m) Timothy, E.; Cloutier, T. E.; Widom, J. *Mol. Cell* **2004**, *14*, 355. (n) Du, Q.; Smith, C.; Shiffeldrim, N.; Vologodskaia, M.; Vologodskii, A. *Proc. Natl. Acad. Sci. U.S.A.* **2005**, *102*, 5397.

(2) For example, see: (a) Shimada, J.; Yamakawa, H. *Macromolecules* **1984**, *17*, 689. (b) Zhang, Y.; Crothers, D. M. *Biophys. J.* **2003**, *84*, 136.

(3) For example, see: (a) Seeman, N. C. *Nature* **2003**, *421*, 33. (b) Winfree, E.; Liu, F.; Wenzler, L. A.; Seeman, N. *Nature* **1998**, *394*, 539. (c) Rothemund, P. *Nature* **2006**, *440*, 297. (d) He, Y.; Ye, T.; Su, M.; Zhang, C.; Ribbe, A. E.; Jiang, W.; Mao, C. *Nature* **2008**, *452*, 198. (e) Douglas, S. M.; Dietz, H.; Liedl, T.; Högberg, B.; Graf, F.; Shih, W. M. *Nature* **2009**, *459*, 414. (f) Zheng, J.; Birktoft, J. J.; Chen, Y.; Wang, T.; Sha, R.; Constantinou, P. E.; Ginell, S. L.; Mao, C.; Seeman, N. C. *Nature* **2009**, *459*, 414. (g) Han, D.; Pal, S.; Nangreave, J.; Deng, Z.; Liu, Y.; Yan, H. *Science* **2011**, *332*, 342. (h) Yin, P.; Hariadi, R. F.; Sahu, S.; Choi, H. M. T.; Park, S. H.; LaBean, T. H.; Reif, J. F. *Science* **2008**, *321*, 824. (i) Iinuma, R.; Ke, Y.; Jungmann, R.; Schlichthaerle, T.; Woehrstein, J. B.; Yin, P. *Science* **2014**, *344*, 65.

(4) Chen, J. H.; Seeman, N. C. *Nature* **1991**, *350*, 631.

(5) Zhang, Y. W.; Seeman, N. C. *J. Am. Chem. Soc.* **1994**, *116*, 1661.

(6) Mao, C. D.; Sun, W. Q.; Seeman, N. C. *Nature* **1997**, *386*, 137.

(7) Goodman, R. P.; Schaap, I. A. T.; Tardin, C. F. C.; Erben, M.; Berry, R. M.; Schmidt, C. F.; Turberfield, A. J. *Science* **2005**, *310*, 1661.

(8) He, Y.; Tian, Y.; Chen, Y.; Deng, Z.; Ribbe, A. E.; Mao, C. *Angew. Chem.* **2005**, *117*, 6852.

(9) Qian, H.; Tian, C.; Yu, J.; Guo, F.; Zheng, M.; Jiang, W.; Dong, Q.; Mao, C. *Small* **2013**, *10*, 855.

(10) Ackermann, D.; Schmidt, T. L.; Hannam, J. S.; Purohit, C. S.; Heckel, A.; Famulok, M. *Nat. Nanotechnol.* **2010**, *5*, 436.

(11) Aldaye, F. A.; Lo, P. K.; Karam, P.; McLaughlin, C. K.; Cosa, G.; Sleiman, H. F. *Nat. Nanotechnol.* **2009**, *72*, 349.

(12) (a) Ma, Y.; Zheng, H.; Wang, C.; Yan, Q.; Chao, J.; Fan, C.; Xiao, S. J. *J. Am. Chem. Soc.* **2013**, *135*, 2959. (b) Zheng, H.; Ma, Y.; Xiao, S. J. *Chem. Commun.* **2014**, *50*, 2100.

(13) Zhang, D. Y.; Seelig, G. *Nature Chem.* **2011**, *3*, 103.

(14) Lu, C. H.; Willner, B.; Willner, I. *ACS Nano* **2013**, *7*, 8320.